



cambridge.org/mrf

Burak Uzman<sup>1</sup>, Adem Yilmaz<sup>1</sup> , Hulusi Acikgoz<sup>1</sup>  and Raj Mittra<sup>2,3</sup>

<sup>1</sup>Department of Electrical and Electronics Engineering, KTO Karatay University, Konya, Turkey; <sup>2</sup>Department of Electrical and Computer Engineering, University of Central Florida, Orlando, Florida, USA and <sup>3</sup>KAU, Jeddah, Saudi Arabia

## Research Paper

**Cite this article:** Uzman B, Yilmaz A, Acikgoz H, Mittra R (2021). Graphene-based microwave coaxial antenna for microwave ablation: thermal analysis. *International Journal of Microwave and Wireless Technologies* **13**, 497–505. <https://doi.org/10.1017/S1759078720001361>

Received: 5 March 2020  
Revised: 30 August 2020  
Accepted: 2 September 2020  
First published online: 19 October 2020

### Keywords:

Microwave cancer ablation; coaxial antenna; backward heating; surface current suppression; graphene

### Author for correspondence:

Hulusi Acikgoz,  
E-mail: [hulusi.acikgoz@karatay.edu.tr](mailto:hulusi.acikgoz@karatay.edu.tr)

### Abstract

In this study, the problem of backward heating in microwave ablation technique is examined and an electromagnetic solution based on the use of high impedance graphene material is presented for its mitigation. In this context, a one-atom-thick graphene layer is added on the coaxial double slot antenna. In addition to the electromagnetic behavior, thermal effects caused by the graphene-covered antenna are emphasized. The graphene's conductivity being highly dependent on its chemical potential and the relaxation time, a parametric study is performed to determine a range of tolerances within which the graphene-coated antenna outperform a typical graphene-free antenna. The range of values is found to be  $0 < \mu_c < 0.5$  eV and  $\tau < 0.4$  ps, for the chemical potential and the relaxation time, respectively. The backward heating problem being prevented, the ablation region is ensured to be spherical around the tip of the antenna. Effects of the graphene layer to the heat dissipation in the tissue, the necrotic tissue ratio (damage to the cancerous tissue of the caused by electromagnetic energy), and the treatment time using the coaxial double slot antenna were examined. The results show that the heat dissipation is concentrated around the slots (region of cancerous tissue) and a higher necrotic tissue ratio can be achieved with a graphene-covered double slot antenna in a shorter time.

## Introduction

The microwave ablation (MWA) technique has gained considerable attention in recent years due to its advantages over its counterparts [1]. MWA is based on the use of microwaves to eradicate cancerous biological tissues by generating heat within the unhealthy ones [2]. MWA is carried out at high frequencies and there is no need of grounding to propagate electromagnetic waves through the tissue [3]. In addition, MWA gives the desired temperature values in a shorter time when compared to the other common technique; namely radiotherapy ablation [4]. MWA is achieved by microwave coaxial antennas (MCA), which operates at 2.45 GHz and can transmit high power into the cancerous tissue [5]. MCAs, such as monopole [6], dipole [7], slot [8, 9], and triaxial [10] are preferred in MWA due to their properties such as easy to design and low return loss [11]. Although MCAs are successful in eradicating the tumor, they exhibit backward heating phenomenon along the antenna, hence they cause damage to the healthy tissue, which is one of the serious problems limiting the use of microwaves as an ablation technique. The reason for the backward heating is the backward surface current, which originates from the slots and propagates along the antenna [12]. In order to reduce the backward heating problem, there have been numerous studies in the literature. These studies have mainly focused on redesigning the antennas by adding “choke” and/or “sleeve” on the antenna. The operating principle of choked [13, 14], cap-choked [15], double choked [16], and sliding choke [17] antennas is to add a metallic structure on the outer conductor of the antenna to obtain an open circuit along the outer conductor. In sleeve [18] and floating sleeve [19] antenna designs, it is aimed to prevent backward surface currents by creating a high impedance structure on the outer conductor of the antenna. Although, all mentioned designs reduce the backward heating to some extent, the dimensions of the antenna become impractical to be implemented in MWA. Readers of the present manuscript should be aware that other techniques based on coating the outer conductor with high loss absorbing materials [20, 21] may give similar results when compared to the results obtained with our graphene-based structure. However, it should be noted that the possibility of using a one-atom thick graphene sheet with extraordinary electronic properties is an important feature for a minimally invasive cancer ablation that is not always achievable by other materials. Although, the growth of a parameter-controlled graphene sheet is still challenging, in the near future, technological progress will certainly permit having more predictable and controlled graphene materials that can be used in similar applications.

In this study, a double slot coaxial antenna coated with one-atom-thick graphene, which behaves as a high impedance surface at microwave frequencies, is considered as a solution to mitigate the backward heating problem. The idea was first proposed by Acikgoz and Mittra [3] where an electromagnetic analysis of the proposed design was performed. In this paper, first, an overview of the electronic properties of the graphene sheet and a parametric study aiming to examine the dependence of its conductivity on the chemical potential and the relaxation time is performed. Then, the analysis of graphene coated antenna is extended to thermal analysis and the study of the tissue damage rate. The numerical results indicate that the backward surface current is considerably mitigated while keeping the dimension of the antenna unchanged. It is also observed that the minimum healthy tissue damage can be obtained with the graphene-coated antenna.

### Graphene-coated microwave antenna

Mechanical exfoliation of graphite [22], the chemical vapor deposition (CVD) [23], exfoliation of carbon nanotubes [24], thermal decomposition [25] are among the most widely used techniques for the growth of the 2D graphene layer. More often, the CVD is the preferred one due to its easiness and the possibility to tune different parameters such as chamber temperature/pressure, gas flow rate, etc., to control the quality of the graphene deposition. The graphene layer can be grown on a copper foil sheet and then transferred on a targeted substrate. To transfer the graphene, it is first spin coated with polymethyl methacrylate (PMMA), followed with drops of polymethyl siloxane. Then the copper foil is removed by placing copper/graphene/PMMA in aqueous iron chloride solution to leave only graphene and PMMA. Finally, graphene/PMMA is transferred to a targeted surface and then the PMMA is dissolved in acetone [26]. Alternatively, authors in [27] have directly grown graphene film on a cylindrical copper conductor as in our case.

The conductivity of the graphene is given by the Kubo's formula [28]:

$$\sigma(\omega) = \frac{2e^2 k_b T}{\pi \hbar} \ln \left( 2 \cosh \frac{\mu_c}{2e^2 k_b T} \right) \frac{j}{\omega + j\tau^{-1}} \quad (1)$$

where  $\tau$  is the relaxation time,  $\mu_c$  is the chemical potential,  $k_b$  is the Boltzmann constant,  $\hbar$  is the Planck constant,  $T$  is the room temperature in Kelvin,  $\omega$  is the angular frequency, and  $e$  is the electron charge. The conductivity of the graphene mainly depends on the applied frequency  $\omega$ , the chemical potential  $\mu_c$ , and the relaxation time  $\tau$ . The modeling of the graphene sheet is explained in detail in reference [16] where it is also shown that the graphene sheet can provide very high impedance as a function of the chemical potential. This behavior can also be seen in Fig. 1(a).

In fact, charge carriers may be induced in the graphene by the application of an electric field or by chemical doping. In the case of the application of an electric field an electric potential between graphene and a substrate is applied. By changing this gate voltage, carrier's concentration in graphene can be tuned. As a result, this induces a change in the chemical potential of the graphene. The second approach based on the chemical doping of the graphene involves either the use of surface adsorbates or to substitute carbon atoms in the graphene layer

by foreign atoms. In the latter case, depending on the type of the incorporated atoms n-type or p-type doped graphene can be obtained [29]. In order to obtain a high impedance surface with low conductivity and to be able to suppress the backward surface current as much as possible, the chemical potential of the graphene should be as close as possible to  $\mu_c = 0$  eV (Fig. 1(a)). However, our designed antenna requires having the graphene layer right on the outer conductor of the coaxial applicator. As such, it is not possible in practice to tune the chemical potential via a gate voltage and therefore, it is unlikely to have 0 eV after deposition. As a consequence, the deposited graphene layer is more prone to have a higher value for its chemical potential leading to a lower surface impedance. As shown in Fig. 1(b), the graphene is also highly dependent on the relaxation time which represent the required time to restore a uniform charge density after a charge distortion is introduced in a material [30]. The variation of graphene's conductivity versus the relaxation time is presented in Fig. 1(b). The relaxation time depends, among others, on the carrier mobility which in turn depends on the quality of the graphene [30]. Large values of the carrier mobility involve having high quality of material with low defects (large relaxation time) whereas low values imply a material with high defects (low relaxation time). Consequently, changing the relaxation time of the graphene by adding defects would be an alternative strategy to change its conductivity. As stated in [28], values for the relaxation time found in the literature range from 0.01 to 1 ps. As mentioned above, these values correspond to the cases where the graphene layer has high and low defects, respectively. In practice, the deposited graphene layer will not be perfect and it will usually present defects which will lower its relaxation time. Therefore, the relaxation time is expected to be in between these values. To see the effect of these two parameters, i.e. the chemical potential and the relaxation time on the performance of the graphene-coated MCA, we have computed the surface current on the outer conductor of the coaxial antenna and the specific absorption rate (SAR) in the liver tissue (along the antenna) for different chemical potentials and relaxation times. In addition, this parametric study will provide us a range of values of these parameters in which the performance of the examined antenna is still improved compared to the graphene-free MCA. This is particularly important because, besides our inability to tune chemical potential via a gate voltage, the deposition of a graphene layer with a precise relaxation time value is challenging and unpredictable. The results are presented in "Electromagnetic analysis".

The designed MCA coated with a one-atom-thick graphene layer inserted in liver tissue is shown in Fig. 2. For hygienic and guidance purposes, the antenna is coated with a polytetrafluoroethylene material called catheter. The 3 mm length slots are positioned between 2–5 and 7–10 mm from the shorted end of the antenna. The physical properties of the materials involved in the model are selected from several literature [19, 31–33] and they are summarized in Table 1.

### Electromagnetic analysis

The effect of the one-atom-thick graphene on the efficiency of MCA is numerically investigated first. The efficiency is calculated as the power radiated into the biological tissue (liver) over the input power received by the coaxial antenna. The graphene-free MCA gives an efficiency of 94%. Hence, it is aimed in this

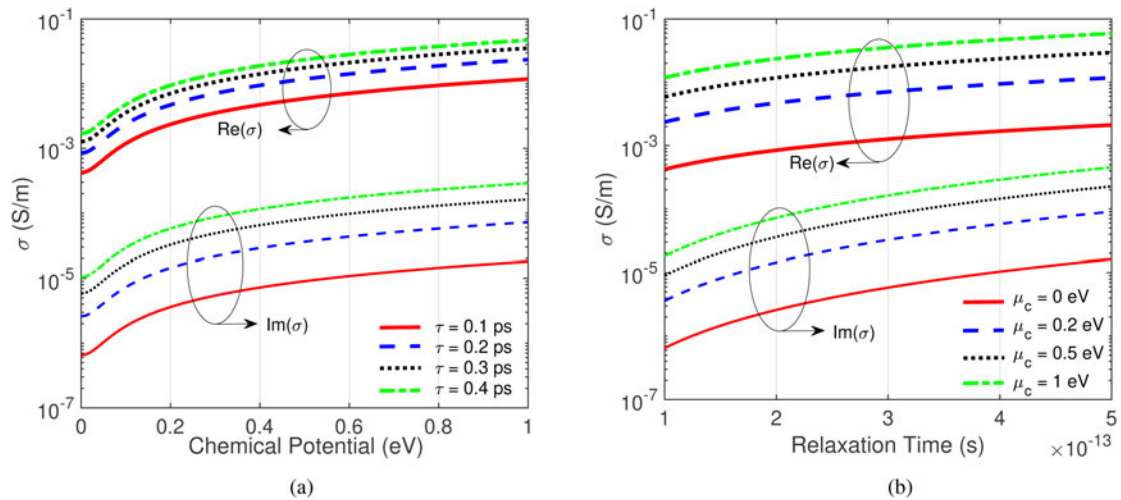


Fig. 1. Conductivity versus chemical potential for different relaxation time (a), Conductivity versus relaxation time for different chemical potential (b).

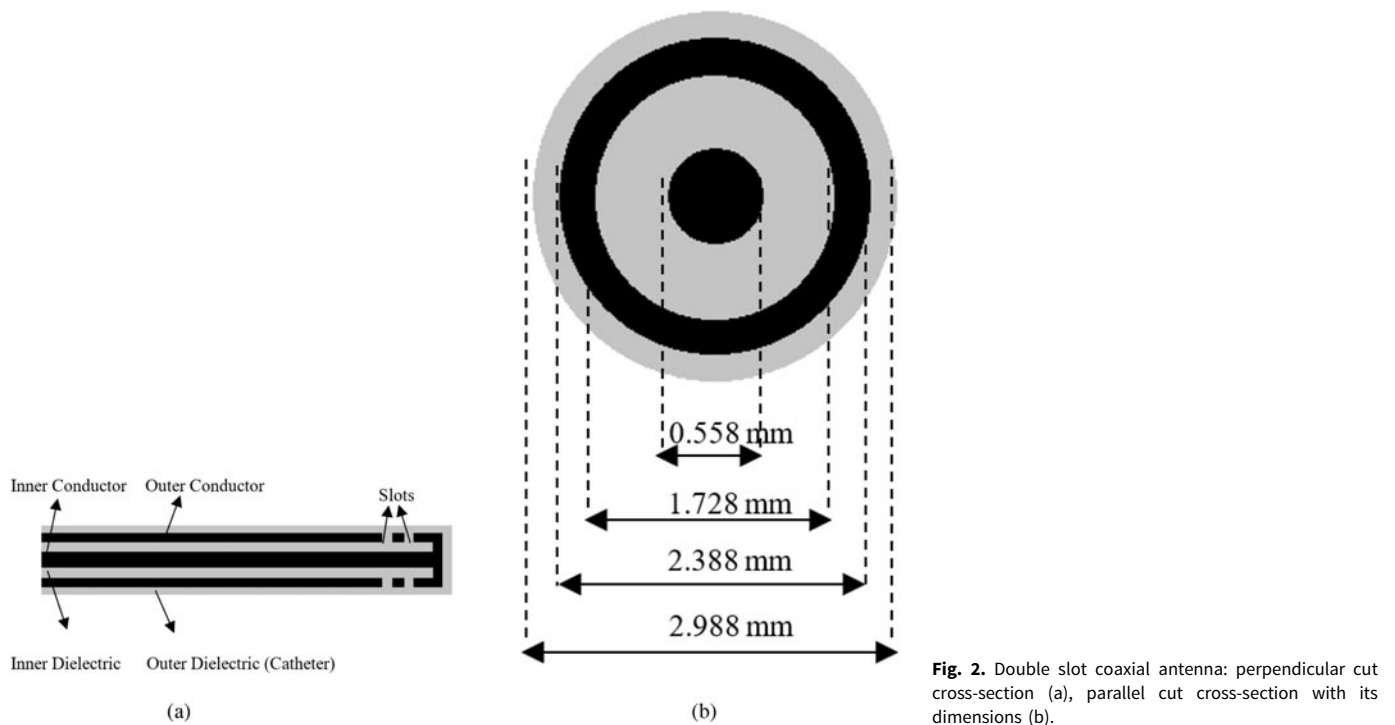


Fig. 2. Double slot coaxial antenna: perpendicular cut cross-section (a), parallel cut cross-section with its dimensions (b).

Table 1. Tissue and antenna parameters

Parameter	Symbol	Value	Unit
Relative permittivity of liver	$\epsilon_{liver}$	43.03	
Electrical conductivity of liver	$\sigma_{liver}$	1.69	S/m
Thermal conductivity of liver		0.512	W/(m·K)
Relative permittivity of inner dielectric		2.03	
Relative permittivity of catheter		2.1	
Operating frequency	$f$	2.45	GHz

study to keep the efficiency of graphene-coated MCA closer to the graphene-free one while reducing the backward surface current. The variation of the efficiency due to the width and the position of the graphene is presented in Fig. 3. It is easily deduced that the efficiency is not affected by the variation of the width of the graphene while keeping its distance to the slot constant (Fig. 3(a)). However, as shown in Fig. 3(b), the efficiency is highly dependent on the position of the graphene, especially when it is placed close to the slot. The lowest efficiency of the MCA is obtained when the graphene sheet is adjacent to the slot. Away from the slot, i.e. after about 20 mm, the efficiency becomes independent of the position. However, as our goal is to reduce the backward heating problem

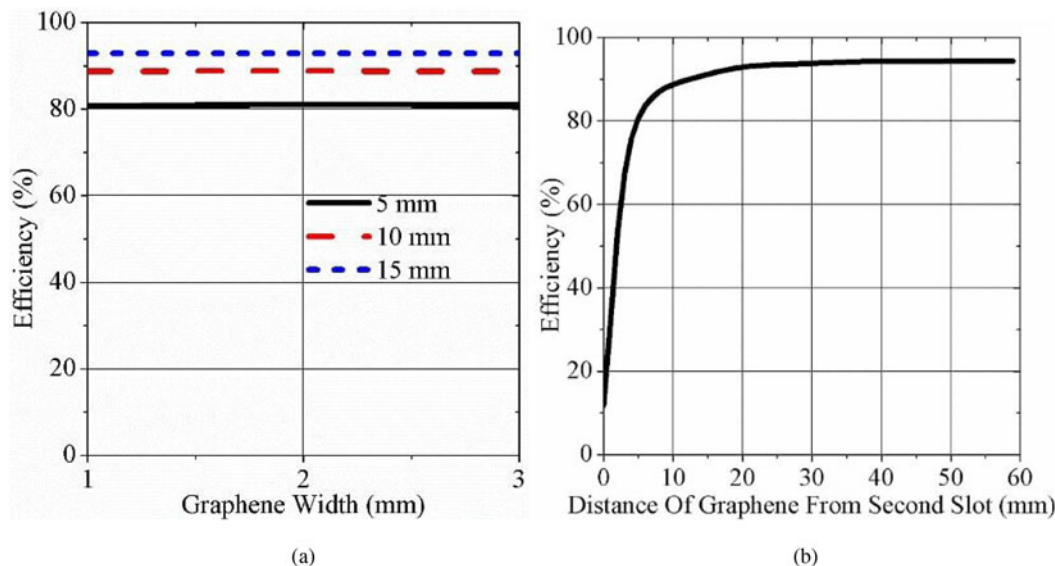


Fig. 3. The effect of length (a) and position (b) of graphene on the efficiency of MCA.

by blocking the propagation of the surface current back to the feed line from the slot, we decided to bring the graphene sheet closer to the slot without lowering the efficiency below 90%. These investigations have resulted in a graphene sheet width of 1 mm positioned at 16 mm from the tip of the MCA. Keeping the width of the graphene sheet as small as possible is important because in practice, larger graphene sheet production would be more difficult and its homogeneity would be at stake [34]. Thus, the overall efficiency of the graphene-coated MCA is calculated to be 90%.

Since the backward heating problem is due to the surface current propagating on the outer conductor of the MCA, the surface currents density with and without graphene sheet is considered. The surface current density on the outer conductor of the MCAs versus the antenna length is depicted in Fig. 5(a). Although the primary effect of adding graphene layer would be to reduce the surface current after the graphene we calculated the surface current density from the slot to the feed line of the antenna, as shown in Fig. 4(a). It is clearly seen that the MCA coated with the 0 eV graphene material has the lowest surface current density when compared with the graphene-free antenna. In addition, 1 eV graphene, which provides lower impedances at microwave frequencies [3], leads to higher surface current density along the antenna when compared with the 0 eV graphene, but this is still low in comparison to the graphene-free antenna. The SAR is evaluated in order to compare the radiation performance of the MCA with and without graphene sheet. The SAR is computed at a radial distance of 1.5 mm from the outer conductor of the MCA (in the liver tissue) and it is depicted in Fig. 5. Two different scenarios are considered. First the relaxation time is kept constant at  $\tau = 0.1$  ps and the SAR is calculated for two different chemical potentials, i.e.  $\mu_c = 0$  eV and  $\mu_c = 1$  eV (Fig. 5(b)). The plot shows that MCA with graphene damps faster than the graphene-free (normal) antenna while the maximum SAR, which should be high around the slot, remains almost the same. As for the surface current, the electromagnetic energy absorbed in the tissue is quickly damped with the 0 eV graphene and the maximum SAR is located around the slots of the

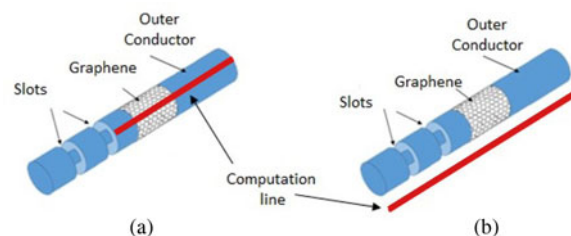
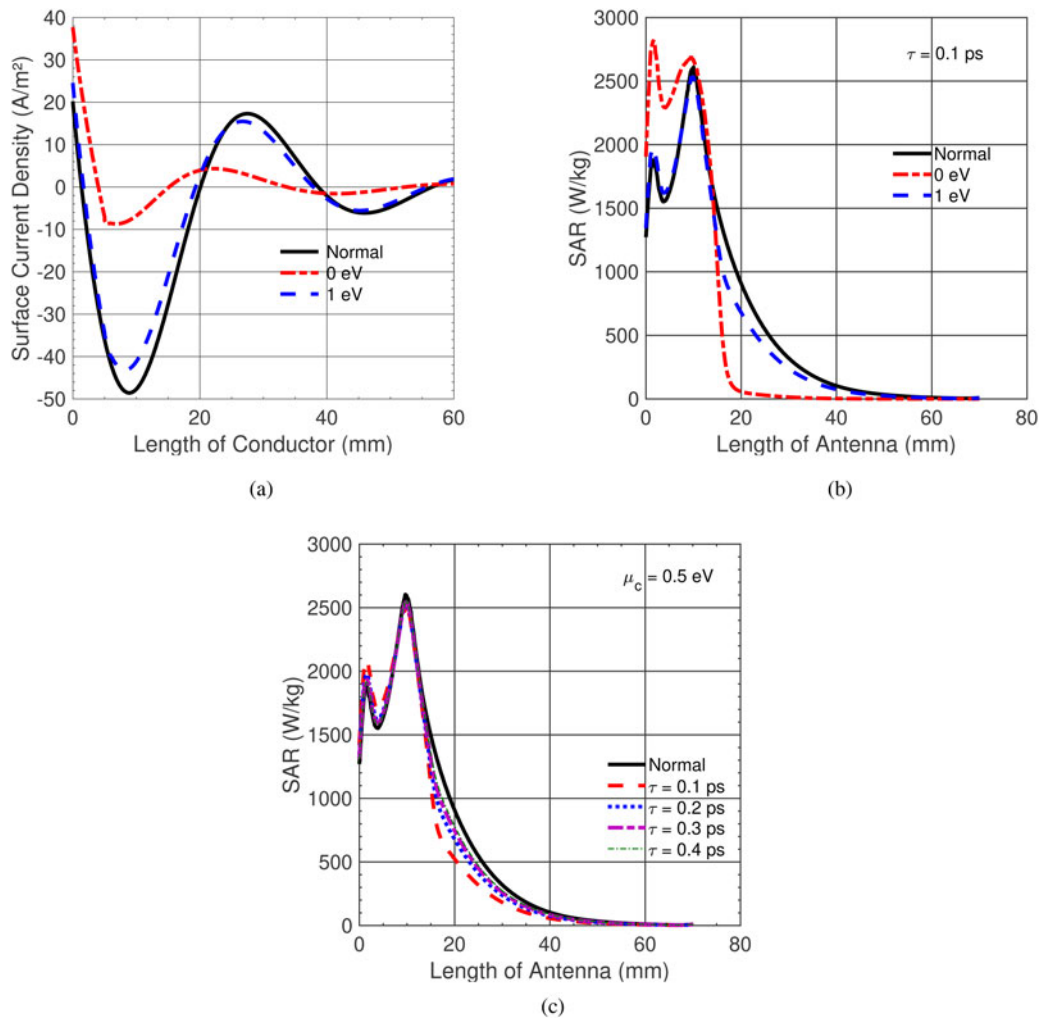


Fig. 4. Picture depicting where on the antenna the surface current is computed (a), picture depicting where the SAR is computed in the tissue (b).

antenna. For a higher chemical potential, i.e. higher conductivity, as expected, the computed SAR is closer to the case without graphene. For the second scenario, we kept the chemical potential constant at  $\mu_c = 0.5$  eV and calculated the SAR for different relaxation times ranging from  $\tau = 0.1$  ps to  $\tau = 0.4$  ps (Fig. 5(c)). We notice that, while being closer to the antenna without graphene, the SAR calculated in the tissue is still low. As higher relaxation times lead to higher conductivities (conversely to lower surface impedances), SARs calculated when the relaxation time increases are getting even closer to those of the graphene-free case. The effect of increasing the relaxation time is similar to increasing the chemical potential via a gate voltage or via chemical doping. Our aim in this parametric study being to provide a range of variation for the chemical potential and the relaxation time, we can deduce that these values should be  $\mu_c < 0.5$  eV and  $\tau < 0.4$  ps, respectively. As previously stated, in practice, growing a graphene sheet with exact properties, i.e. chemical potential and relaxation time are challenging and not predictable. Thus, these values will provide guidelines for researchers working in this area.

In the following subsections, thermal and damaged tissue rate analysis are presented by changing the chemical potential only. Nonetheless, the same analysis may be performed using the relaxation time and the general behavior of the graphene-coated MCA will be similar to those presented hereafter. In





**Fig. 5.** Surface current density along the antenna calculated after the slots and toward the feed line (“normal” refers to the graphene-free antenna) (a) and the SAR all the way along the antenna for different chemical potentials with  $\tau = 0.1$  ps (b) and for different relaxation times with  $\mu_c = 0.5$  eV (c).

fact, as long as these two parameters are below the upper limits given above, we are secured that that performance of the MCA will be improved.

**Thermal analysis**

As the main contribution of this work is to study the thermal effect of the graphene covered antenna on the biological tissue, the temperature distribution is investigated via the use of the Penn’s equation expressed as in equation (2) [35]:

$$\rho C \frac{\partial T}{\partial t} = \nabla(k_{th} \nabla T) + \omega_b \rho_b C_b (T_b - T) + Q_{met} + Q_{ext}. \quad (2)$$

The tissue parameters in the Penn’s equation are shown in Table 2. The generation of heat by the electric field is expressed in equation (3).

$$Q_{ext} = \frac{1}{2} \sigma_{liver} |\vec{E}|^2. \quad (3)$$

The relationship between the electric field, SAR and surface current is expressed in equations (4) and (5).

$$SAR = \frac{\sigma_{liver}}{2\rho} |\vec{E}|^2. \quad (4)$$

$$\vec{j} = \sigma \vec{E}. \quad (5)$$

Thus, the Penn’s equation can be directly related to the SAR as follow:

$$\rho C \frac{\partial T}{\partial t} = \nabla(k_{th} \nabla T) + \omega_b \rho_b C_b (T_b - T) + Q_{met} + \rho SAR. \quad (6)$$

The temperature distribution in liver tissue at a radial distance of 1.5 mm away from the MCA is calculated and given in Fig. 6. It is observed that, in accordance with the SAR distribution, the antenna with 0 eV graphene coating gives the highest temperatures at around the slots and it decreases instantly to the low temperatures along the antenna, which indicates that the highest

temperature can be delivered to the tissue at around the slots while keeping the minimum damage to the tissue along the antenna. This idea can be best explained when the damaged tissue ratio is examined.

### Damaged tissue due to electromagnetic energy absorption

Several mechanisms have been proposed for describing the biological tissue damage due to the elevation of the temperature. For instance, a simple model based on multiplying the elevation of temperature  $\Delta T$  by the time for holding this high temperature is considered [36]. This model has been proven to be inefficient to model tissue damage correctly. A more specific model based on calculating an equivalent time at a reference temperature, where a cell damage is observed, is also considered. The model used in this paper has been largely used in the hyperthermia community. It provides a complex function that relates tissue temperature and time of the temperature elevation to the damaged tissue rate [5, 37]. In this model, the damaged tissue rate is varying exponentially with temperature and linearly with time.

The ratio of the tissue exposed to the electromagnetic energy transferred to the tissue is expressed in equation (7).

$$\Omega(t) = \ln \left( \frac{c(0)}{c(t)} \right) = \int_0^t A e^{-\Delta E/RT} dt. \quad (7)$$

In equation (7),  $\Omega(t)$  is necrotic tissue rate,  $c(t)$  is live cell density,  $c(0)$  is live cell density before ablation,  $R$  is universal gas constant,  $A$  frequency factor ( $s^{-1}$ ),  $\Delta E$  activation energy for irreversible damage reaction (J/mol) [38]. It is straightforward from the equation (7) that as the duration of ablation increases the total integral value i.e. the damaged tissue rate increases. indicates that tissue necrosis has occurred. This critical value corresponds to 37% live tissue density, i.e. 63% tissue death [39].

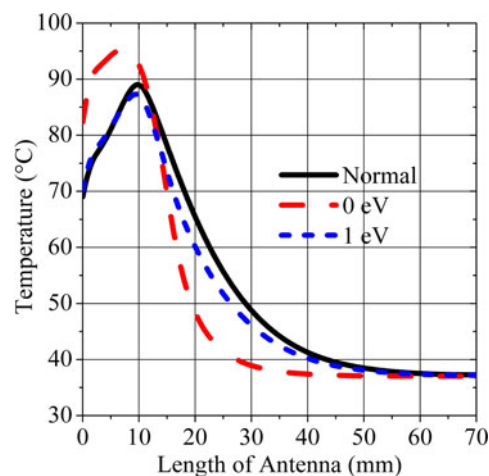
The necrotic tissue rate being defined as above, this latter is computed in the tissue between the slots and after the graphene position (Fig. 7). It can be seen from Fig. 8(a) that MCA with 0 eV graphene coating reaches higher temperature in a shorter time with 100% of tissue damage rate compared to the other types of MCA (Fig. 8(b)). On the other hand, one can deduce from Fig. 9(a) that relatively low temperature increase is obtained beyond the 0 eV graphene coated MCA while having minimum tissue damage (Fig. 9(b)).

Figure 10 shows a 2D distribution of the damaged tissue ratio (necrotic tissue ratio) caused by the electromagnetic energy radiated from the graphene-free and 0 eV graphene-coated MCAs. It can be easily observed that the backward reaction phenomenon is significantly reduced with respect to the graphene-free antenna. Thus, healthy tissue is prevented from damage throughout the antenna and a more spherical ablation zone around the slots is achieved.

Finally, the sleeve and choke antennas, which are widely used in MWA to reduce surface currents and thus to minimize backward heating, have been modeled in order to compare the performance of the proposed antenna graphene coated with  $\mu_c = 0$  eV,  $\tau = 0.1$  ps. The dimensions and material properties of single slot sleeve and choke antennas are obtained from the papers [18, 19]. The comparison between antennas is performed in terms of SAR (Fig. 11(a)) and temperature (Fig. 11(b)) distributions along the antennas. In contrast to these antenna structures, the graphene-coated MCA concentrates more the energy around

**Table 2.** Tissue parameters in penn equation

Parameter	Symbol	Value	Unit
Tissue density	$\rho$	1060	kg/m <sup>3</sup>
Specific tissue temperature	$C$	3600	J/kg·K
Tissue temperature	$T$	37	°C
Thermal conductivity	$k_{th}$	0.512	W/(m·K)
Blood density	$\rho_b$	1000	kg/m <sup>3</sup>
Specific blood heat	$C_b$	4180	J/kg·K
Blood perfusion rate	$\omega_b$	$3.6 \cdot 10^{-3}$	s <sup>-1</sup>
Metabolic heat energy	$Q_{met}$	33,800	W/m <sup>3</sup>



**Fig. 6.** Temperature distribution in the tissue along the antenna.

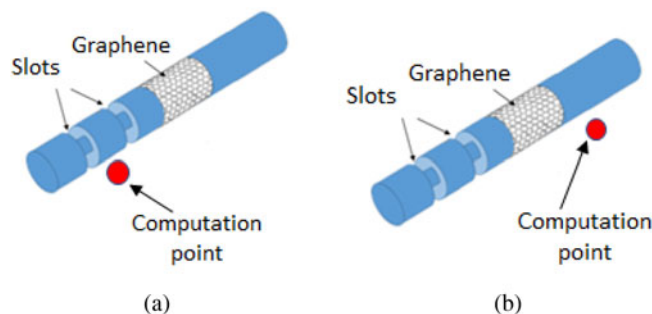


**Fig. 7.** Pictures depicting where the necrotic tissue rate is computed in the tissue, between the slots (a), after the graphene (b).

the slots and damps immediately right after the slots. Hence the healthy tissue along the antenna is prevented from damage and a more spherical ablation zone around the slots is achieved with the proposed graphene-based antenna (Fig. 12).

### Conclusion

In this paper, a novel structure based on the use of a 2D material namely graphene as a high impedance surface for mitigating the propagation of surface currents on the outer conductor of a

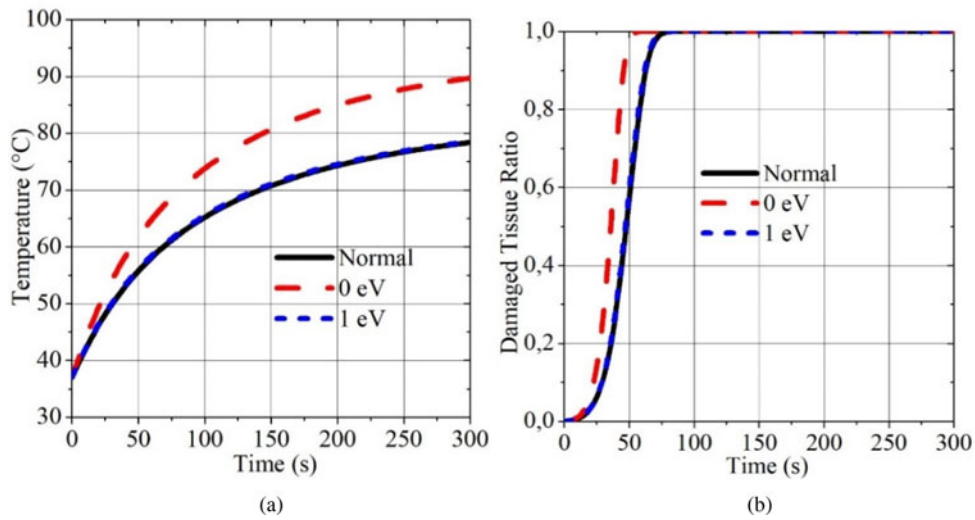


Fig. 8. Temperature distribution (a), tissue damaged rate (b), at a 1.5 mm distance, between slots.

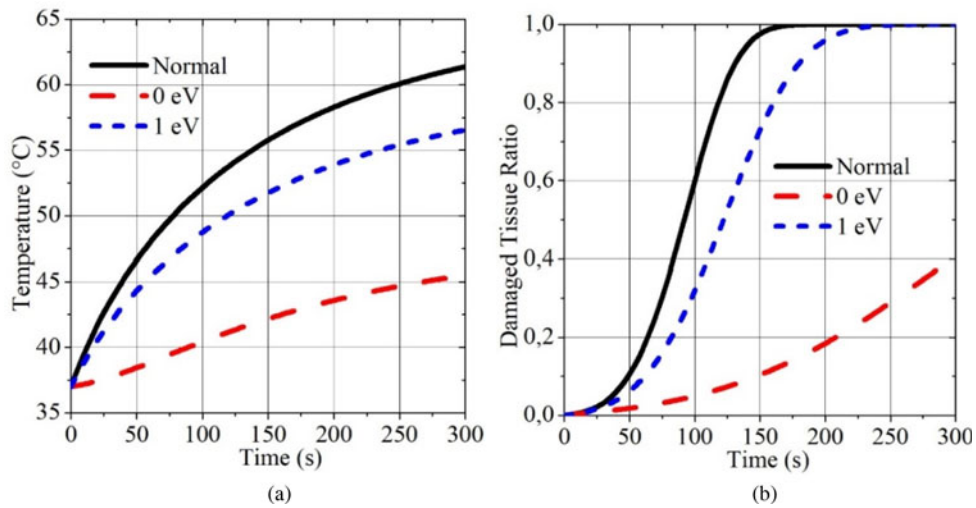


Fig. 9. Temperature versus time (a), tissue damaged rate (b), computed at a radial distance of 1.5 mm, after the graphene.

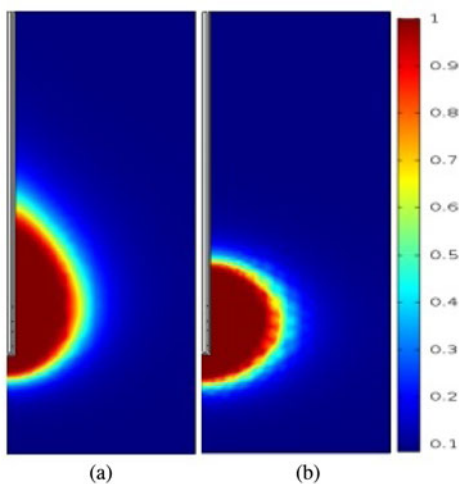


Fig. 10. 2D damage tissue rate: without graphene (a), with 0 eV graphene-coated antenna (b).

MCA has been presented and some numerical results have been discussed. A parametric study has been carried out to find a range of values for the chemical potential and the relaxation time. It is concluded that, the chemical potential and the relaxation time of the graphene should be  $\mu_c < 0.5$  eV and  $\tau < 0.4$  ps in order to have substantial improvement in comparison to the performance of the graphene-free antenna. Furthermore, a thermal analysis of the structure demonstrated that the antenna covered with a graphene layer is capable of reducing surface currents and thus decreasing the elevation of the temperature in healthy tissue. Consequently, a more spherical ablation zone may be obtained with the application of the microwave heating antenna. Moreover, due to the restriction of the temperature elevation only in the unhealthy tissue region, a rapid tissue necrosis is observed. Graphene-coated antenna is also compared with some common structures to address this problem such as choke and sleeve antennas. Results are encouraging in such a way that the proposed antenna outperforms the ones given in the literature.

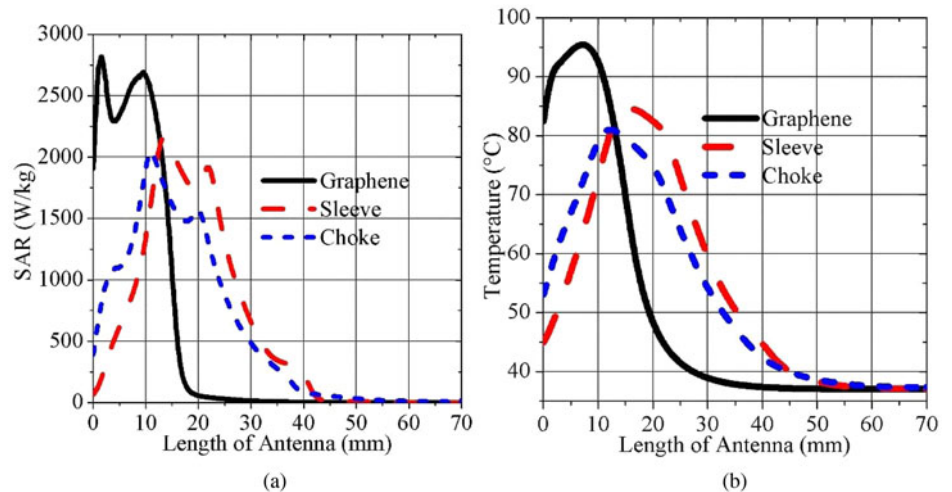


Fig. 11. SAR distribution (a), Temperature distribution (b), at 1.5 mm distance from antennas.

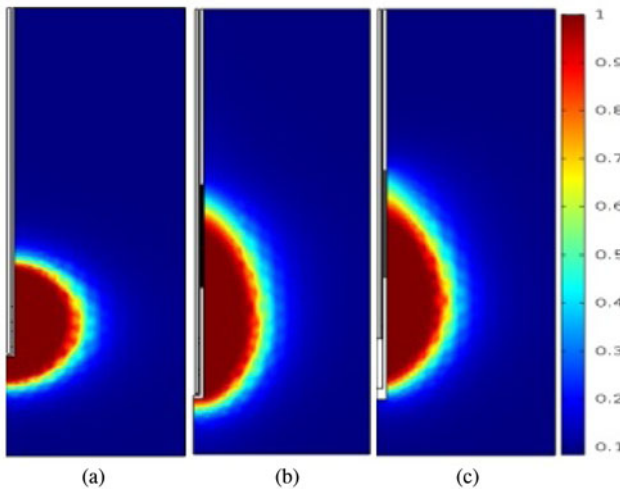


Fig. 12. 2D damaged tissue ratio: 0 eV Graphene (a), Choke (b), Sleeve (c).

Experimental works are needed to confirm the results presented in this paper before possible clinical trials.

**Acknowledgement.** The authors would like to thank the support from the Scientific and Technological Research Council of Turkey (TUBITAK) ARDEB-3001 Grant No: 116E298.

## References

- Yang D (2006) *Measurements, Antenna Design And Advanced Computer Modelling For Microwave Tissue Ablation* (dissertation). University of Wisconsin–Madison.
- Rubio MF, Hernandez AV, Salas LL, Navarro EA and Navarro EA (2011) Coaxial slot antenna design for microwave hyperthermia using finite-difference time-domain and finite element method. *Open Nanomedicine Journal* 3, 2–9.
- Acikgoz H and Mittra R (2016) Suppression of surface currents at microwave frequency using graphene- application to microwave cancer treatment. *Applied Computational Electromagnetics Society Journal* 31, 669–677.
- Brace CL (2009) Radiofrequency and microwave ablation of the liver, lung, kidney, and bone: what are the differences? *Current Problems in Diagnostic Radiology* 38, 135–143.
- Prakash P (2010) Theoretical modeling for hepatic microwave ablation. *The Open Biomedical Engineering Journal* 4, 27–38.
- Labonte S, Blais A, Legault SR, Ali HO and Roy L (1996) Monopole antennas for microwave catheter ablation. *IEEE Transactions on Microwave Theory and Techniques* 44, 1832–1840.
- Hurter W, Reinbold F and Lorenz WJ (1991) A dipole antenna for interstitial microwave hyperthermia. *IEEE Transactions on Microwave Theory and Techniques* 39, 1048–1054.
- Keangin P, Rattanadecho P and Wessapan T (2011) An analysis of heat transfer in liver tissue during microwave ablation using single and double slot antenna. *International Communications in Heat and Mass Transfer* 38, 757–766.
- Wongtrairat W, Phasukkit P, Tungjikusolmun S and Nantivatana P (2011) The effect of slot sizes on non-asymmetry slot antenna for microwave coagulation therapy. *International Journal of Bioscience, Biochemistry and Bioinformatics* 1, 192–198.
- Brace CL, Van Der Weide DW, Lee FT and Laeseke PF (2004) Analysis and experimental validation of a triaxial antenna for microwave tumor ablation. Paper presented at: 2004 IEEE MTT-S International Microwave Symposium Digest; June 6–11; Fort Worth, TX, USA.
- Bertram JM, Yang D, Converse MC, Webster JG and Mahvi DM (2006) A review of coaxial-based interstitial antennas for hepatic microwave ablation. *Critical Reviews™ in Biomedical Engineering* 34, 187–213.
- Acikgoz H and Turer I (2014) A novel microwave coaxial slot antenna for liver tumor ablation. *Advanced Electromagnetics* 3, 1–20.
- Longo I, Gentili GB, Cerretelli M and Tosoratti N (2003) A coaxial antenna with miniaturized choke for minimally invasive interstitial heating. *IEEE Transactions on Biomedical Engineering* 50, 82–88.
- Lara JE, Vera A, Leija L and Gutierrez MI (2015) Modeling of electromagnetic and temperature distributions of an interstitial coaxial-based choked antenna for hepatic tumor microwave ablation. Paper presented at: 12th International Conference on Electrical Engineering, Computing Science and Automatic Control (CCE); October 28–30; Mexico City, Mexico.
- Lin JC and Wang YJ (1996) The cap-choke catheter antenna for microwave ablation treatment. *IEEE Transactions on Biomedical Engineering* 43, 657–660.
- Acikgoz H and Mittra R (2015) Microwave coaxial antenna for cancer treatment: Reducing the backward heating using a double choke. Paper presented at: 2015 International Symposium on Antennas and Propagation, ISAP 2015; November 9–12; Hobart, TAS, Australia.
- Prakash P, Converse MC, Webster JG and Mahvi DM (2009) An optimal sliding choke antenna for hepatic microwave ablation. *IEEE Transactions on Biomedical Engineering* 56, 2470–2476.
- Prakash P, Deng G, Converse MC, Webster JG, Mahvi DM and Ferris MC (2008) Design optimization of a robust sleeve antenna for hepatic microwave ablation. *Physics in Medicine and Biology* 53, 1057–1069.
- Yang D, Bertram JM, Converse MC, O'Rourke AP, Webster JG, Hagness SC, Will JA and Mahvi DM (2006) A floating sleeve antenna



- yields localized hepatic microwave ablation. *IEEE Transactions on Biomedical Engineering* **53**, 533–537.
20. Li Y, Li D, Wang X, Nie Y and Gong R (2018) Influence of the electromagnetic parameters on the surface wave attenuation in thin absorbing layers. *AIP Advances* **8**, 056616.
  21. Chen HY, Deng LJ, Zhou PH, Xie JL and Zhu ZW (2011) Improvement of surface electromagnetic waves attenuation with resistive loading. *Progress in Electromagnetics Research Letters* **26**, 143–152.
  22. Novoselov KS, Geim AK, Morozov SV, Jiang D, Zhang Y, Dubonos SV, Grigorieva IV and Firsov AA (2004) Electric field effect in atomically thin carbon films. *Science* **306**, 666.
  23. Somani PR, Somani SP and Umeno M (2006) Planer nanographenes from camphor by CVD. *Chemical Physics Letters* **430**, 56.
  24. Cano-Márquez AG, Rodríguez-Macías FJ, Campos-Delgado J, Espinosa-González CG, Tristán-López F, Ramírez-González D, Cullen DA, Smith DJ, Terrones M and Vega-Cantú YI (2009) Ex-MWNTs: graphene sheets and ribbons produced by lithium intercalation and exfoliation of carbon nanotubes. *Nano Letters* **9**, 1527.
  25. Vázquez de parga AL, Calleja F, Borca B, Passeggi Jr MCG, Hinarejos JJ, Guinea F and Miranda R (2008) Periodically rippled graphene: growth and spatially resolved electronic structure. *Physical Review Letters* **100**, 056807.
  26. Syarifah Norfaezah S, Shafiq Hafly S, Siti Fazlina F, Meghashama Lim CK and Noraini O (2017) Graphene transfer process and optimization of graphene coverage. *EPJ Web of Conferences* **162**, 01049.
  27. Datta AJ, Gupta B, Shafiei M, Taylor R and Motta N (2016) Growth of graphene on cylindrical copper conductors as an anticorrosion coating: a microscopic study. *Nanotechnology* **27**, 285704.
  28. Llatser I, Kremers C, Chigrin D, Jornet JM, Lemme MC, Cabellos-Aparicio A and Alarc Supón E (2012) Radiation characteristics of tunable graphennas in the terahertz band. *Radioeng J* **21**, 946–953.
  29. Pinto H and Markevich A (2014) Electronic and electrochemical doping of graphene by surface adsorbates. *Beilstein Journal of Nanotechnology* **5**, 1842–1848.
  30. Abadal S, Hosseininejad SE, Lemme MC, Bolívar PH, Solé-Pareta J, Alarcón E and Cabellos-Aparicio A (2020) *Nanoscale Networking and Communications Handbook, Chapter 2*. Boca Raton, USA: CRC Press.
  31. Bertram JM, Yang D, Converse MC, Webster JG and Mahvi DM (2006b) Antenna design for microwave hepatic ablation using an axisymmetric electromagnetic model. *BioMedical Engineering Online* **5**, 1–9.
  32. Yang D, Converse MC, Mahvi DM and Webster JG (2007) Expanding the bioheat equation to include tissue internal water evaporation during heating. *IEEE Transactions on Biomedical Engineering* **54**, 1382–1388.
  33. Jacobsen S and Stauffer PR (2007) Can we settle with single-band radio-metric temperature monitoring during hyperthermia treatment of chest-wall recurrence of breast cancer using a dual-mode transceiving applicator? *Physics in Medicine and Biology* **52**, 911–928.
  34. Orofeo CM, Ago H, Hu B and Tsuji M (2011) Synthesis of large area, homogeneous, single layer graphene films by annealing amorphous carbon on Co and Ni. *Nano Research* **4**, 531–540.
  35. Jiao T, Wang H, Zhang Y, Yu X, Xue H, Lv H, Jing X, Zhan H and Wang J (2012) A coaxial-slot antenna for invasive microwave hyperthermia therapy. *Journal of Biomedical Science and Engineering* **5**, 198–202.
  36. Dewey WC and Diederich CJ (2009) Hyperthermia classic commentary: “Arrhenius relationships from the molecule and cell to the clinic”. *International Journal of Hyperthermia* **25**, 21–24.
  37. Chang IA (2010) Considerations for thermal injury analysis for RF ablation devices. *The Open Biomedical Engineering Journal* **4**, 3–12.
  38. Borrelli MJ, Thompson LL, Cain CA and Dewey WC (1990) Time-temperature analysis of cell killing of BHK cells heated at temperatures in the range of 43.5°C to 57.0°C. *International Journal of Radiation Oncology Biology Physics* **19**, 389–399.
  39. Chang IA and Nguyen UD (2004) Thermal modeling of lesion growth with radiofrequency ablation devices. *BioMedical Engineering Online* **3**, 1–19.



**Burak Uzman** received the B.S. and M.S degrees in electrical and electronics engineering from the KTO Karatay University, Konya, Turkey. He is currently working as an antenna engineer at Engitek Ltd. His research interests include antennas for microwave cancer and antennas for mobile communication.



**Adem Yilmaz** received the B.S. and M.S degrees in electrical and electronics engineering from the University of Gaziantep and Ankara Yildirim Beyazit University, respectively. He is currently pursuing the Ph.D. degree at Ankara Yildirim Beyazit University, Turkey. From 2010 to 2011, he was a researcher at Goethe Frankfurt University, Germany. Since 2011, he has been a Research Assistant at KTO Karatay University. His research interests include design and characterization of periodic structures, antennas for microwave cancer, computational electromagnetics, and the theory of characteristic modes.



**Hulusi Acikgoz** received the B.S. and Master degrees in applied physics from the Paris-Est Marne-La-Val Supée University, France, and the Ph.D. degree from the Pierre and Marie Curie University (UPMC-Paris IV), Paris, France, in 2008 in electrical engineering. He has been a teaching assistant at UPMC-Paris IV in 2009–2010. After a year of post-doctoral research at the L2E (Laboratoire d'Electronique et d'Electromagn Supétisme) in computational electromagnetic dosimetry, he joined the KTO Karatay University, Konya, Turkey, in 2011, as an assistant professor. He spent a year as visiting scholar with Dr. Raj Mittra's research group at Pennsylvania State and Central Florida Universities, USA. His research interests include microwave characterization of dielectric materials, electromagnetic dosimetry, homogenization, antennas for microwave cancer ablation, high impedance surfaces, graphene applications in EM, and statistical analysis of EM structures.



**Raj Mittra** (LF'96) was a Professor of electrical and computer engineering, Penn State, State College, PA, USA, from 1996 to 2015. He was a Professor with the Electrical and Computer Engineering, University of Illinois at Urbana-Champaign, Champaign, IL, USA, from 1957 to 1996. He is currently a Professor with the Department of Electrical Engineering and Computer Science, University of Central Florida, Orlando, FL, USA, where he is currently the Director with the Electromagnetic Communication Laboratory. He is currently the Hi-Ci Professor with King Abdulaziz University, Jeddah, Saudi Arabia. Mittra was a recipient of the Guggenheim Fellowship Award in 1965, the IEEE Centennial Medal in 1984, the IEEE Millennium medal in 2000, the IEEE/AP-S Distinguished Achievement Award in 2002, the Chen-To Tai Education Award in 2004 and the IEEE Electromagnetics Award in 2006, and the IEEE James H. Mulligan Award in 2011. He is a PastPresident of AP-S, and he has served as the Editor of the Transactions of the Antennas and Propagation Society. He founded the e-Journal FERMAT and has been serving as the co-editor-in-chief of the same. He is a Principal Scientist and President of RM Associates, a consulting company founded in 1980, which provides services to industrial and governmental organizations, both in the USA and abroad.